A Mathematical Model for the Evaluation of Airborne Infection Risk for Bus Passengers

Jenjira Sooknum, and Nopparat Pochai

Abstract—**Human breath emits a lot of carbon dioxide, which contributes a lot to airborne infections. Airborne infections spread speedily, and breathing can expose us to life-threatening airborne infections. There is a risk of infection if people are traveling by bus. A mathematical model of carbon dioxide concentration measurement due to human breath is proposed in this research. The focus of this research is to determine the amount of carbon dioxide produced by bus passengers. The model's solution is approximated using an explicit finite difference technique. The model solution can be used to determine how much time passengers are willing to spend on the bus while carbon dioxide levels are kept under control. Furthermore, mathematical models were utilized to quantify the risk of air infection among bus passengers with ventilation systems, in order to reduce the risk of air infection and increase ventilation. The proposed air quality model was found to be in good agreement in that it allows us to know the balance between the number of passengers allowed to sit on the bus while managing the risk of airborne infection, carbon dioxide concentration, and ventilation system potential. A significant advantage of the ventilation will be better air quality control that balances the number of passengers permitted to ride on a bus.**

Index Terms—**Airborne, Bus, Finite difference technique, Mathematical model, Passengers**

I. Introduction

THEY focus on three epidemiological models for predicting the spread of airborne infections in confined areas [14]. The basic formulation of Gammiatoni and Nucci is demonstrated to be the best for simulating airborne transmission in ventilated spaces, and it is then utilized in parametric research to assess the effect of physical and environmental factors on disease transmission rates. They used a deterministic mathematical model for airborne transmission to estimate the efficacy of proposed tuberculosis (TB) infection control strategies [5]. As the infectivity of the source case grows, the effectiveness of these control measures reduces. They monitored carbon dioxide levels in classrooms under non-steady state settings [4].

Manuscript received June 30, 2022; revised November 4, 2022.

This work was supported in part by the Centre of Excellence in Mathematics, Ministry of Higher Education, Science, Research and Innovation, Bangkok, Thailand.

J. Sooknum is a Ph.D. student in Applied Mathematics, Department of Mathematics, Faculty of Science, King Mongkut's Institute of Technology Ladkrabang, Bangkok, 10520, Thailand (e-mail: jr.sooknum@gmail.com).

N. Pochai is an Associate Professor of Department of Mathematics, Faculty of Science, King Mongkut's Institute of Technology Ladkrabang, Bangkok, 10520, Thailand (corresponding author to provide phone: 662329-8400; fax: 662-329-8400; e-mail: nop_math@yahoo.com).

A carbon dioxide-based risk equation was used to evaluate tuberculosis transmission criteria. With such a high smear positive rate, the idea of producing carbon dioxide levels of 1000 ppm by natural ventilation assists in meeting WHO criteria for providing healthy indoor environments for children and controlling the TB epidemic in high-prevalence locations. They used a carbon dioxide decay technique to measure ventilation in air changes per hour (ACH) using the Wells-Riley equation to estimate TB transmission risk in traditional households [10]. When the windows were closed at baseline, low ventilation was discovered, indicating a high risk of TB spreading. They review and critically evaluate current building ventilation strategies to assess the state of the art and elaborate on whether there is room for further development, particularly in high-occupancy buildings, to reduce or eliminate pathogen transmission risk and adapt ventilation measures in [24].

They devised a handheld carbon dioxide meter in [18], which they paired with social contact diary recordings to estimate daily rebreathed liters. They then calculated the daily amounts of air rebreathed by teenagers in a densely populated area. They show how to quantify the carbon dioxide levels to which people are exposed in a series of non-constant indoor situations. A new metric for rebreathed air volume takes into account social and environmental aspects linked to airborne infection and can be used to pinpoint areas with high transmission potential. They propose in [1] that they estimated the risk of tuberculosis transmission on three modes of public transportation using a modified Well-Riley model for airborne transmission of infection and exhaled carbon dioxide as a natural tracer gas to evaluate air exchange using a modified Well-Riley model for airborne disease transmission. Public transportation, with its poor ventilation and high respiratory contact rates, may play a significant role in sustaining tuberculosis transmission.

They investigated [16] according to personal categorization. There are four types of people who stay in an outpatient room: patients, patient relatives, workers, and visitors. The intake and output ventilation rates are adjusted to simulate air quality control procedures in the presence of a number of individuals. The model solution was approximated using the fourth-order Runge-Kutta method. In an outpatient room, the suggested numerical model can be utilized to simulate the dynamic dispersion of airborne infectious diseases. The model's results will allow for the control of airborne infection in increasingly complex structures. They developed a model [22] that sets the carbon dioxide concentration at any point when the number of people and ventilation rate change. To approximate the

model solution, the fourth-order Runge-Kutta method is used. In the presented simulations, there are numerous scenarios for improving air quality. The proposed model balances the number of people allowed to stay in the room with the capacity of the air ventilation system in the air quality management process. They develop and demonstrate a flexible mathematical model [21] that monitors exhaled air by infectors in a limited environment to estimate the risk of airborne infectious diseases such as tuberculosis in steady and non-steady state situations. They demonstrated a mathematical and detailed design connection between the probability of TB transmission and the rate of airborne infection particle generation, the ventilation rate, the average volume percentage of exhaled air, the prevalence of TB, and the length of time of infector exposure in a fixed space. [27] provides a mathematical model for calculating the risk of airborne infection in a room with an outlet ventilation system. The air quality control system's proposed model achieves a compromise between the number of people who are allowed to stay in the space and the effectiveness of the ventilation system. A risk model of airborne transmission and vaccine effectiveness in an outpatient room with a ventilation system is proposed in [28]. This research might be put to use to help lower the risk of airborne infection to the appropriate level if there was a public vaccination database system.

How can we determine the risk of airborne infection at that location at that time if there is an epidemic of infectious diseases in the air or at a place where there are affected people? In this study, we utilized a mathematical approach to calculate the risk of airborne infection among passengers on buses with a ventilation system.

A. BUS STRUCTURE

The dimensions of the car are 2.5 meters wide, 2.5 meters high and 12 meters long as shown in Figure 1.

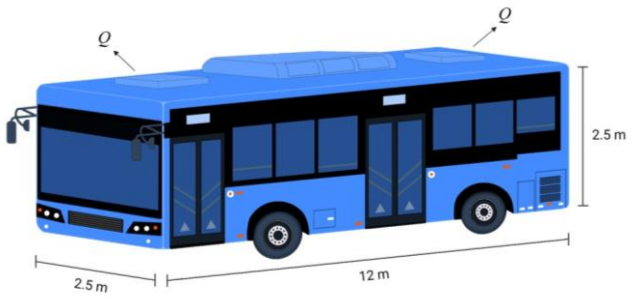

Fig.1. A bus model.

The 48-seater air-conditioned bus is shown in the seat map in Figure 2. and has two exhaust fans at the front and rear of the bus.

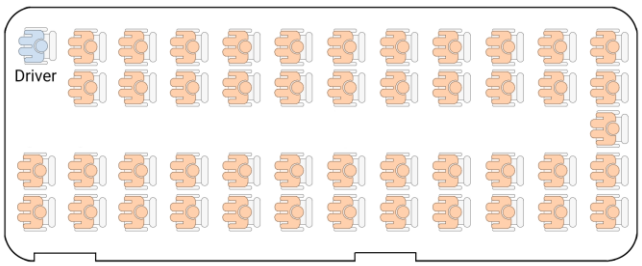

Fig.2. Seat map.

II. GOVERNING EQUATION

The rate of exhaled air emission and ventilation per person, in general, influences the increased concentration of indoor carbon dioxide [6, 8, and 9]. Carbon dioxide levels can be used as an exhaled air replacement since an infected individual's exhaled air contains airborne infectious particles [4], [6], [7], [9], and [18]. Carbon dioxide levels in the atmosphere are typically around 400 parts per million [3], [4], and [6].

A. A one-dimensional exhaled air concentration measurement model: a bus with a constant number of passengers

We assume that a bus interior space, such as a bus with a volume of V. Given the presence of infectors, the concentration of exhaled air that may contain airborne contagious particles may tend to rise in the bus, based on the rate of ventilation Q, and the number of people in the bus.

The advection-diffusion equation can be used to model a variety of environmental issues such as [29], [30], [31], [32], [33], [34], [35] and [36]. We simply assume that passengers on the bus contribute significantly to carbon dioxide production, which acts as an exhaled air marker. The exhaled air rate generated by passengers plus the carbon dioxide diffusion rate, minus the ventilation rate that removes exhaled air, is the primary equation of the accumulation rate of exhaled air concentration in a bus with carbon dioxide:

$$\frac{\partial C}{\partial t} = D\frac{\partial^2 C}{\partial x^2} + npC_a - QC\,, \tag{1}$$

for all $(x,t) \in \Omega$, where $\Omega = [0,L]\times[0,T]$, C is the concentration of air inside the exhaled bus (ppm), p is the rate of breathing (L/s) for each person in the bus and C_a is the carbon dioxide fraction included in breathed air, t is the duration time, T is the stationery simulation time and L is the length of a considered bus. Initial condition $C(x,0) = C_0$ where C_0 is the latent carbon dioxide concentration. The boundary conditions are given by $\frac{\partial C}{\partial x} = C_F$ where $x = 0$ and C_F is a given constant, and $\frac{\partial C}{\partial x} = C_B$ where $x = L$ and C_B is a given constant.

B. A one-dimensional exhaled air concentration measurement model: a bus with a variable number of passengers

In a simple scenario, if a number of people are unstable, then the number of people depends on the time assumed by $n(x,t)$. In this study, we preferred to use (1) as follows:

$$\frac{\partial C}{\partial t} = D\frac{\partial^2 C}{\partial x^2} + n(x,t)pC_a - QC\,, \tag{2}$$

for all $(x,t) \in \Omega$.

C. The volume fraction of exhaled air

We obtain the concentration of sampled exhaled air, $C(x,t)$, in the given space. By the volume fraction of exhaled air, $f(x,t)$, given by the concentration of sampled air divided by the carbon dioxide fraction included in breathed air, we get

$$f(x,t)=\frac{C(x,t)}{C_a}, \tag{3}$$

for all $(x,t)\in\Omega$.

D. The concentration of airborne infectious particles

If airborne infectious particles generated by infectors reach the target infection site of the host at a threshold level, the probability of infection for susceptible individuals are exceedingly high [15]. Some infectious particles, on the other hand, can get stuck in the upper respiratory tract and spread to other parts of the body. Let β be the total airborne infectious particles generation rate released by an infector (particles/s) and μ be the mortality rate of generated airborne infectious particles by the infector that do not reach the alveolar (particles/s).

The concentration of airborne infectious particles, N, that cause infection, is equal to the volume fraction of rebreathed air by infectors multiplied by the concentration of airborne infectious particles generated by infectors in the space that reach the respiratory tract's target infection site:

$$N(x,t)=\frac{If(x,t)(\beta-\mu)}{n(x,t)p},\ I\geq 1 \text{ and } \beta-\mu\geq 1, \tag{4}$$

where I is the number of infectors in the bus and for all $(x,t)\in\Omega$.

E. The number of airborne infectious particles

Because not all infectious particles can reach and deposit in the alveoli, let θ represent the respiratory deposition fraction of airborne infectious particles that successfully reach and deposit at the host's target infection location. As a result, the number of airborne infectious particles, $\lambda(x,t)$, inhaled by a susceptible individual that cause infection is equal to the product of the volume of air inhaled by the susceptible, the respiratory deposition fraction of airborne infectious particles, θ, which is greater than zero but less than 1, and the concentration of airborne infectious particles released by infectors,

$$\lambda(x,t)=pt\theta N(x,t), \tag{5}$$

where t is the time spent in the space up to the point of infection and for all $(x,t)\in\Omega$.

F. The risk of airborne infection

The probability of airborne infection risk for susceptible individuals:

$$P(x,t)=1-e^{-\lambda(x,t)}, \tag{6}$$

where $(x,t)\in\Omega$.

III. NUMERICAL TECHNIQUES

A continuous approximation to the solution $C(x,t)$ will not be obtained; instead, approximations to C will be generated at various values, called mesh point, in the interval $[0,T]$.

Once the approximate solution at other points in the interval can be found by interpolation. We first make the stipulation that the mesh points are equally distributed throughout the interval $[0,T]$. This condition is ensured by choosing a positive integer M and selecting the mesh point $t_n=n\mathrm{l}$, for each $n=0,1,2,...,M$ where $\mathrm{l}=(T-0)/M$ is called the time step. This condition is ensured by choosing a positive integer N and $x_m=mh$, for each $m=0,1,2,...,N$. The common distance between the points $h=(L-0)/N$ is called the step size.

A. Initial condition setting

$$C(x,0)=f(x), \tag{7}$$

for all $(x,t)\in\Omega$ and $f(x)$ is a given function of the remained exhaled air concentration in an empty bus.

B. Boundary conditions setting

Assuming that there is no absorbance mechanism on the front and the back of the considered bus. The left boundary condition (LBC):

$$\frac{\partial C}{\partial x}=C_F, \tag{8}$$

for all $t>0$ and $x=0$.

The right boundary condition (RBC):

$$\frac{\partial C}{\partial x}=C_B, \tag{9}$$

for all $t>0$ and $x=L$.

C. A forward-time centered-space finite difference method for A one-dimensional exhaled air concentration measurement model: a bus with a variable number of passengers

Retaining in $\frac{\partial u}{\partial t}$ and $\frac{\partial^2 u}{\partial x^2}$ in (2).

Letting that

$$C\approx C_m^n, \tag{10}$$

$$C_m^n=C(x_m,t_n), \tag{11}$$

$$C_{m+1}^n=C(x_m+h,t_n), \tag{12}$$

$$C_m^{n+1}=C(x_m,t_n+\mathrm{l}), \tag{13}$$

$$C_{m-1}^n=C(x_m-h,t_n), \tag{14}$$

then

$$\frac{C_m^{n+1}-C_m^n}{\mathrm{l}}=D\left(\frac{C_{m-1}^n-2C_m^n+C_{m+1}^n}{h^2}\right)+n(x,t)pC_a-QC_m^n,$$

$$C_m^{n+1}=\frac{D\mathrm{l}}{h^2}\left(C_{m-1}^n-2C_m^n+C_{m+1}^n\right)+n(x,t)pC_a\mathrm{l}-QC_m^n\mathrm{l}+C_m^n,$$

$$C_m^{n+1}=\alpha C_{m-1}^n-2\alpha C_m^n+\alpha C_{m+1}^n+n(x,t)pC_a\mathrm{l}-QC_m^n\mathrm{l}+C_m^n,$$

from (15), we get the FTCS finite difference equation becomes

$$C_m^{n+1} = \alpha C_{m-1}^n - (2\alpha + Q\mathrm{l} - 1)C_m^n + \alpha C_{m+1}^n + n(x,t)pC_a\mathrm{l}, \quad (15)$$

where $\alpha = \frac{D\mathrm{l}}{h^2}$ is the diffusion number and $p = 0.12$ (L/s) is the breathing rate. The stability condition of (15) is [26] $0 < \alpha \le \frac{1}{2}$.

IV. NUMERICAL EXPERIMENTS AND RESULTS

Assuming that the bus of volume $V = 75$ (m^3), each person's breathing rate in the bus assumed by $p = 0.12$ (L/s), then the diffusion coefficient of carbon dioxide $D = 0.732$ (m^2 /s), the carbon dioxide fraction included in breathed air $C_a = 0.04$ and the rate of change of the carbon dioxide at the frontend and the backend in the bus is neglected which are $C_F = C_B = 0$.

A. *Simulation 1: the probability of airborne infection risk for susceptible individuals on the bus with reduced ventilation rates.*

The number of passengers in each row is shown in Table I. $C_0 = 0.1$ is the initial value of the concentration of carbon dioxide in the air on a bus (ppm) and the bus uses the air vent rate is 75, 37.5, 18.75, 0. We achieve the approximated solutions illustrated in Figure 13 by using the forward time centered space (FTCS) method (10) to (15) and (3) shown in Figure 5.

TABLE I
THE NUMBER OF PASSENGERS ON THE BUS IN EACH ROW.

Time (min)	The number of passengers in each row												
	0	1	2	3	4	5	6	7	8	9	10	11	12
0-10	0	1	1	1	1	1	1	1	1	1	1	1	0
10-20	0	3	3	3	3	3	3	3	3	3	3	3	3
20-30	0	2	4	4	4	4	4	4	4	4	2	2	2
30-40	0	1	1	1	1	1	1	1	1	1	1	1	1
40-50	0	2	2	2	2	2	2	2	2	2	2	2	2
50-60	0	2	2	2	2	2	2	2	2	2	0	0	0

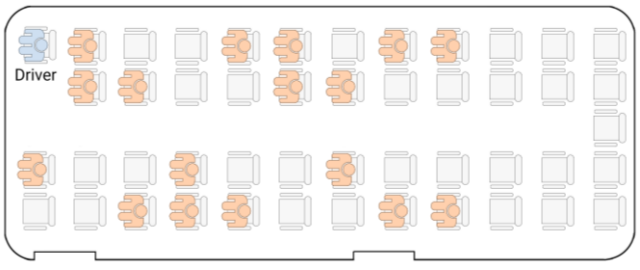

Fig.3. Seat map of the number of people seated on the bus for 50 to 60 minutes.

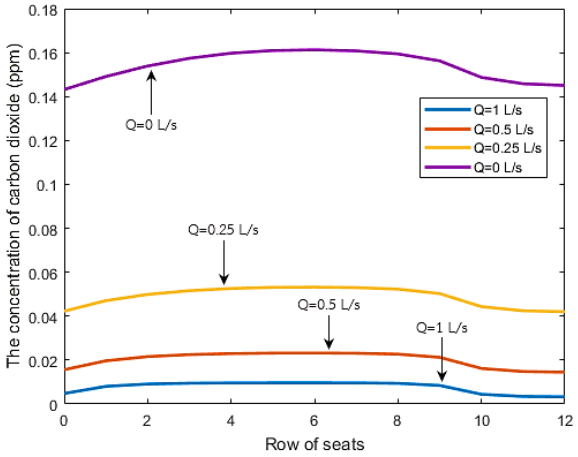

Fig.4. The approximated carbon dioxide concentration in the air on a bus at 60 min with a ventilation system $\mathrm{l} = 0.1$ $T = 60$.

We can see that the concentration of carbon dioxide in the air increases due to the reduced ventilation rate.

TABLE II
THE CONCENTRATION OF CARBON DIOXIDE IN THE AIR ON A BUS AT 60 MIN.

x	The concentration of carbon dioxide			
	$Q = 1$	$Q = 0.5$	$Q = 0.25$	$Q = 0$
0	0.0048	0.0156	0.0423	0.1432
1	0.0080	0.0197	0.0471	0.1491
2	0.0091	0.0216	0.0499	0.1539
3	0.0095	0.0225	0.0516	0.1574
4	0.0096	0.0230	0.0526	0.1597
5	0.0096	0.0232	0.0531	0.1610
6	0.0096	0.0232	0.0532	0.1613
7	0.0096	0.0231	0.0530	0.1608
8	0.0094	0.0227	0.0523	0.1594
9	0.0084	0.0212	0.0503	0.1562
10	0.0044	0.0162	0.0443	0.1487
11	0.0034	0.0148	0.0424	0.1458
12	0.0033	0.0145	0.0420	0.1451

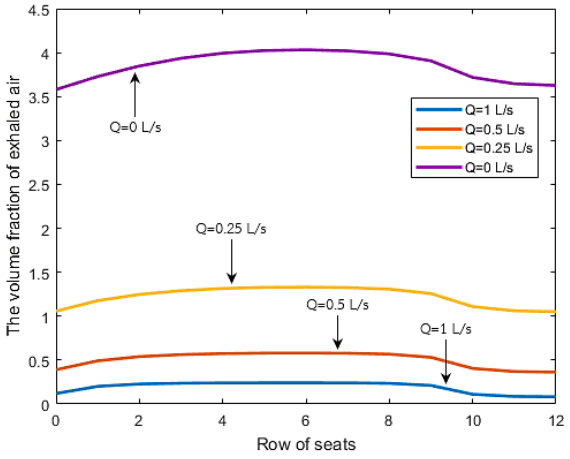

Fig.5. The volume fraction of exhaled air on a bus at 60 min.

We can see that at 60 minutes the fraction of exhaled air volume increases due to the decrease in ventilation rate.

TABLE III
PHYSICAL PARAMETERS.

I	θ	β	μ
1	0.25	100	87

Physical parameters as shown in table III. We achieve the approximated solutions illustrated in Figure 6 to 8 by using (4) shown in Figure 6, (5) shown in Figure 7 and (6) shown in Figure 8.

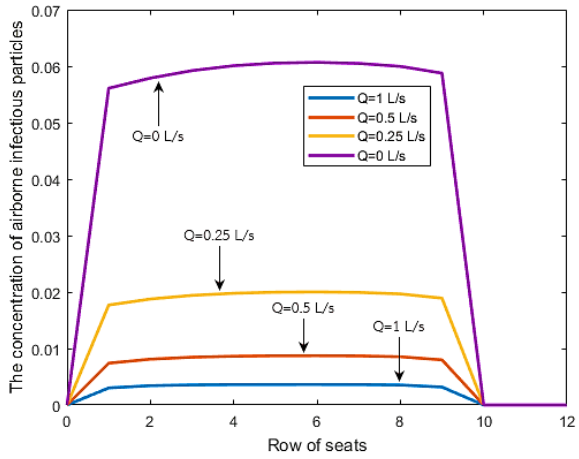

Fig.6. The concentration of airborne infectious particles on a bus at 60 min.

We can see that in 60 minutes, the concentration of airborne infectious particles increases as the respiratory rate decreases.

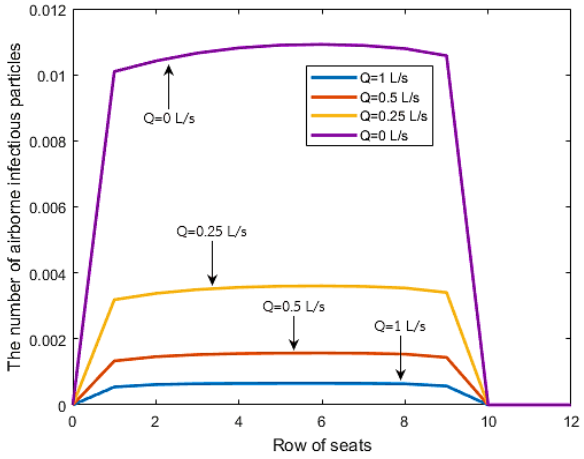

Fig.7. The number of airborne infectious particles on a bus at 60 min.

We can see that in 60 minutes, the number of airborne infectious particles increases as the respiratory rate decreases.

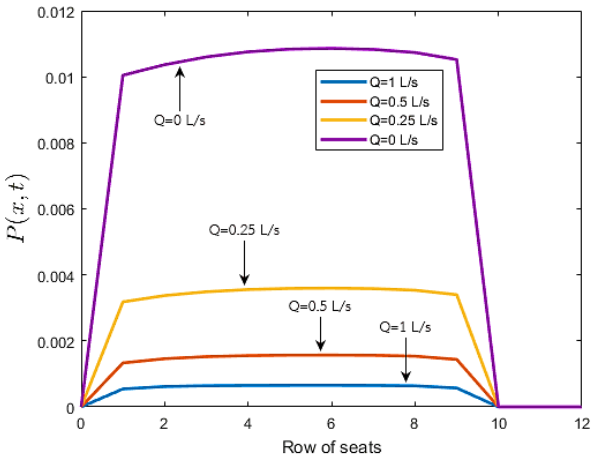

Fig.8. The probability of airborne infection risk for susceptible individuals on a bus at 60 min.

We can see that in 60 minutes, at a ventilation rate of 1 (L/s), the passenger is at the lowest risk of airborne infection.

TABLE IV
THE PROBABILITY OF AIRBORNE INFECTION RISK FOR SUSCEPTIBLE INDIVIDUALS ON A BUS AT 60 MIN.

The probability of airborne infection risk for susceptible individuals				
x	$Q=1$	$Q=0.5$	$Q=0.25$	$Q=0$
0	0	0	0	0
1	0.5435×10^{-3}	0.0013	0.0032	0.0100
2	0.6162×10^{-3}	0.0015	0.0034	0.0104
3	0.6407×10^{-3}	0.0015	0.0035	0.0106
4	0.6493×10^{-3}	0.0016	0.0036	0.0108
5	0.6524×10^{-3}	0.0016	0.0036	0.0108
6	0.6529×10^{-3}	0.0016	0.0036	0.0109
7	0.6505×10^{-3}	0.0016	0.0036	0.0108
8	0.6372×10^{-3}	0.0015	0.0035	0.0107
9	0.5714×10^{-3}	0.0014	0.0034	0.0105
10	0	0	0	0
11	0	0	0	0
12	0	0	0	0

B. ***Simulation 2****: the probability of airborne infection risk for susceptible individuals on the bus.*

Table I lists the number of passengers in each row. $C_0 = 0.1$ is the initial value of carbon dioxide in the air on a bus (ppm) and the bus uses the air vent rate of 75. We achieve the approximated solutions illustrated in Figure 10 to 12 by using the forward time centered space (FTCS) method (10) to (15) and (3) shown in Figure 13.

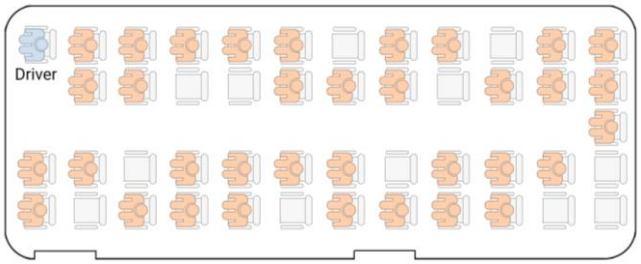

Fig.9. Seat map of the number of people seated on the bus for 10 to 20 minutes.

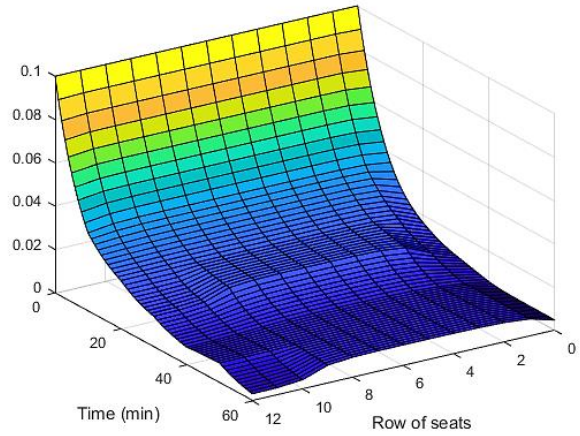

Fig.10. The approximated carbon dioxide concentration in the air on a bus with a ventilation system $l = 0.1$ $T = 60$.

From Figure 10, we can see that the carbon dioxide concentration in the air decreases because there are fewer passengers in each row as passengers get off the bus.

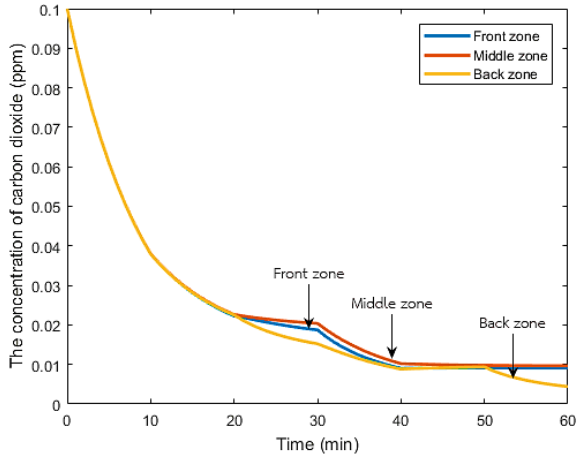

Fig.11. The concentration of carbon dioxide in the air in the front, middle and rear zones on a bus with a ventilation system $l = 0.1$ $T = 60$.

From Figure 11, we can see that the concentration of carbon dioxide in the middle zone is higher than the other zones.

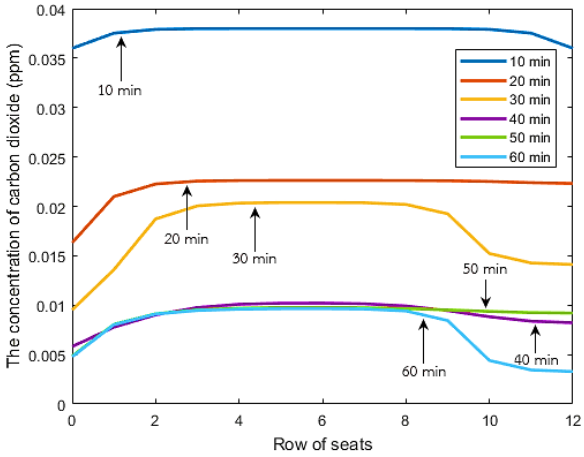

Fig.12. The concentration of carbon dioxide in the air on a bus every 10 minutes with a ventilation system $l = 0.1$ $T = 60$.

From Figure 12, we can see that in the case of a constant ventilation rate, the carbon dioxide concentration in the air decreases sharply with fewer passengers.

TABLE V
THE CONCENTRATION OF CARBON DIOXIDE IN THE AIR ON A BUS EVERY 10 MINUTES.

	The concentration of carbon dioxide					
x	$t=10$	$t=20$	$t=30$	$t=40$	$t=50$	$t=60$
0	0.0360	0.0163	0.0095	0.0058	0.0048	0.0048
1	0.0375	0.0210	0.0136	0.0078	0.0081	0.0080
2	0.0379	0.0223	0.0187	0.0090	0.0091	0.0091
3	0.0380	0.0226	0.0200	0.0098	0.0095	0.0095
4	0.0380	0.0226	0.0203	0.0101	0.0097	0.0096
5	0.0380	0.0226	0.0204	0.0102	0.0098	0.0096
6	0.0380	0.0226	0.0204	0.0102	0.0098	0.0096
7	0.0380	0.0226	0.0204	0.0101	0.0097	0.0096
8	0.0380	0.0226	0.0202	0.0099	0.0097	0.0094
9	0.0380	0.0226	0.0192	0.0094	0.0095	0.0084
10	0.0379	0.0225	0.0152	0.0088	0.0094	0.0044
11	0.0375	0.0224	0.0143	0.0084	0.0092	0.0034
12	0.0360	0.0223	0.0141	0.0082	0.0092	0.0033

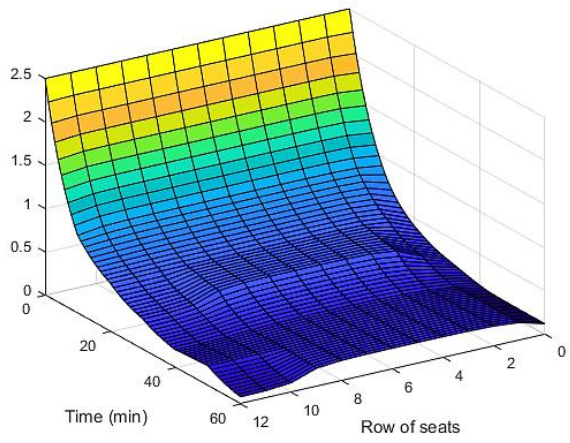

Fig.13. The volume fraction of exhaled air on a bus.

From Figure 13, we can see that the passenger exhaled air volume fraction increases as the number of passengers increases.

Table III lists the physical parameters. We achieve the approximated solutions illustrated in Figure 14 to 18 by using (4) shown in Figure 14, (5) shown in Figure 15, and (6) shown in Figure 16 to 18.

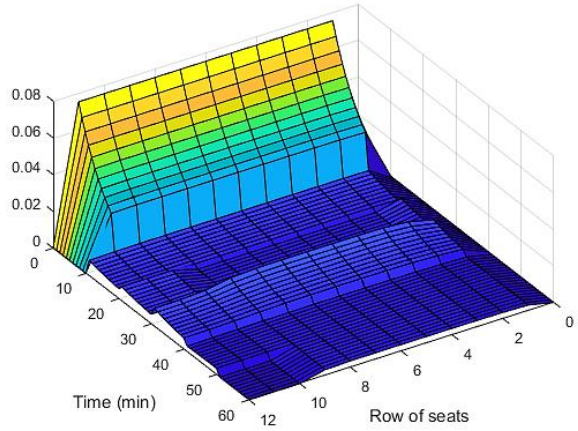

Fig.14. The concentration of airborne infectious particles.

From Figure 14, we can see that the number of passengers at 0 to 10 minutes and at 30 to 40 minutes resulted in higher concentrations of airborne infectious particles than at other points in time.

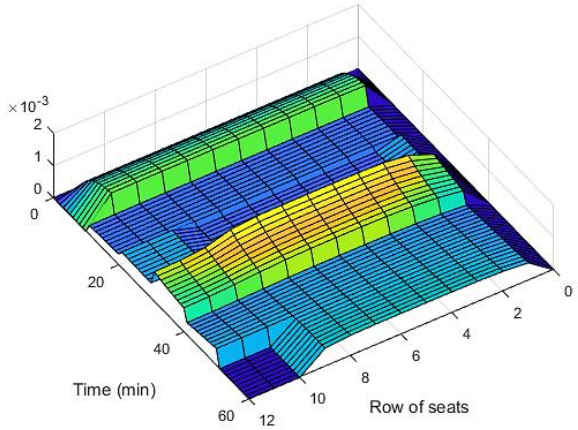

Fig.15. The number of airborne infectious particles.

From Figure 15, we can see that the number of infectious particles in the air at 0 to 10 minutes and 30 to 40 minutes is high due to the low number of passengers.

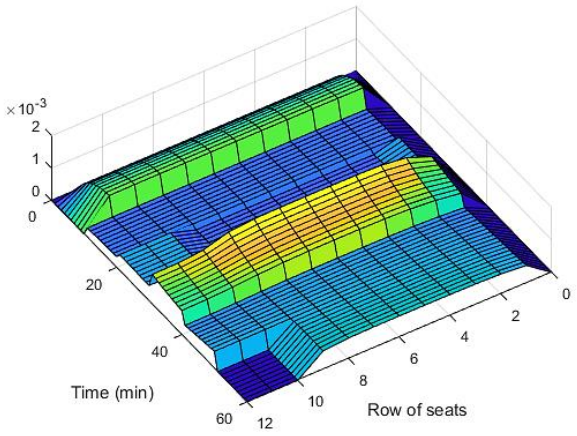

Fig.16. The probability of airborne infection risk for susceptible individuals.

From Figure 16, we can see that passengers seated at 0 to 10 minutes and 30 to 40 minutes are at high risk of airborne infection.

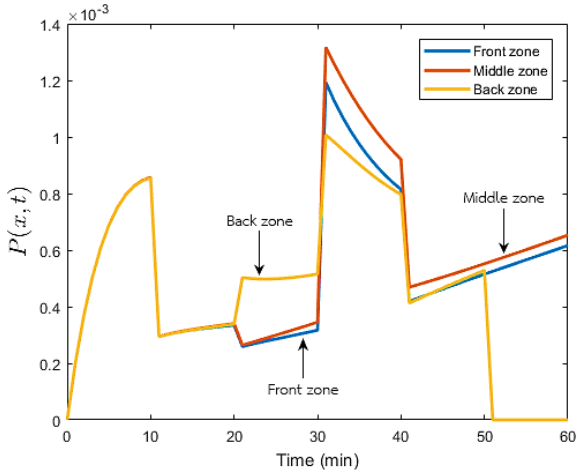

Fig.17. The probability of airborne infection risk for susceptible individuals in the front, middle and rear zones on a bus.

From Figure 17, we can see that the passengers who take a seat in the middle zone have a higher risk than those in other zones.

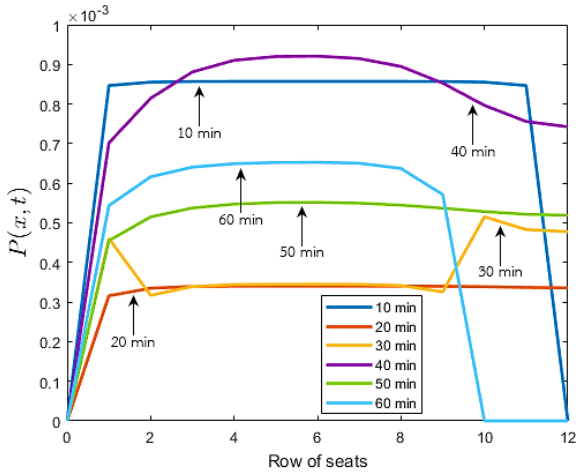

Fig.18. The probability of airborne infection risk for susceptible individuals every 10 minutes.

From Figure 18, we can see that passengers seated for 10 minutes, and 40 minutes are at a high risk of airborne infection.

TABLE VI
THE PROBABILITY OF AIRBORNE INFECTION RISK FOR SUSCEPTIBLE INDIVIDUALS EVERY 10 MINUTES.

The probability of airborne infection risk for susceptible individuals ($\times 10^{-3}$)						
x	$t=10$	$t=20$	$t=30$	$t=40$	$t=50$	$t=60$
0	0	0	0	0	0	0
1	0.8466	0.3158	0.4602	0.7018	0.4550	0.5435
2	0.8552	0.3349	0.3169	0.8145	0.5149	0.6162
3	0.8569	0.3393	0.3392	0.8809	0.5375	0.6407
4	0.8571	0.3402	0.3441	0.9103	0.5472	0.6493
5	0.8571	0.3404	0.3450	0.9199	0.5511	0.6524
6	0.8571	0.3404	0.3451	0.9209	0.5517	0.6529
7	0.8571	0.3404	0.3447	0.9148	0.5496	0.6505
8	0.8571	0.3403	0.3417	0.8948	0.5447	0.6372
9	0.8569	0.3398	0.3257	0.8526	0.5370	0.5714
10	0.8552	0.3387	0.5153	0.7965	0.5283	0
11	0.8466	0.3369	0.4830	0.7559	0.5216	0
12	0	0.3357	0.4777	0.7425	0.5191	0

V. DISCUSSION

As indicated in Table I, we calculated the carbon dioxide concentration in the air on the bus with varied ventilation rates by the number of passengers in each row in simulation 1. Figure 4 shows the carbon dioxide levels after 60 minutes. It is clear that as the ventilation rate lowers, the carbon dioxide concentration rises. Table II shows the approximate carbon dioxide concentration.

Figures 6–8 show the various ventilation rates on the bus after 60 minutes. The volume fraction of exhaled air, the concentration of airborne infectious particles, the quantity of airborne infectious particles, and the probability of airborne infection risk for susceptible individuals all increase as the ventilation rate falls. Table IV shows the probability of receiving an infection from the air for those who are susceptible.

In simulation 2, the number of passengers on the bus in each row is as shown in Table I. When estimated using the forward time-centered space (FTCS) method, the surface graph is obtained as shown in Figure 10. It can be seen that the concentration of carbon dioxide at the starting point decreases and increases gradually from about row 2 to row 10. Over a period of about 10 to 30 minutes, it gradually decreases again as the number of passengers has already disembarked the bus and fewer passengers sit in each row.

From Figure 11, we show the concentration of carbon dioxide in the front, middle, and rear zones of the bus over a period of 60 minutes. It can be seen that the front zone and the middle zone have more passengers than the rear zone. Therefore, the concentration of carbon dioxide in the middle zone is higher than in other zones. That is, each graph increases and decreases corresponding to the number of passengers. The concentration of carbon dioxide in the air on the bus every 10 minutes is shown in Figure 12. Since the ventilation rate is constant, it can be seen that from 0 to 20 minutes there are few bus passengers, thus reducing the concentration of carbon dioxide rapidly.

For 10 to 30 minutes, the number of bus passengers increased, thereby slowing the ventilation, resulting in a gradual decrease in the concentration of carbon dioxide. The approximate carbon dioxide concentration is shown in Table V. From Figure 13, the volume fraction of exhaled air on a bus increases and decreases corresponding to the number of passengers. The physical parameters in Table III are estimated using (4) to (6) as shown in Figures 14 to 18, where we show that when the number of passengers seated in each row is low, the result is the concentration of airborne infectious particles. The number of airborne infectious particles and the probability of airborne infection risk for susceptible individuals increase.

From Figure 16, the front, and the middle zones for 0 to 10 minutes and 30 to 40 minutes clearly show that the probability of airborne infection risk for susceptible individuals increases due to the small number of passengers seated in each row and the rear zone. The probability of airborne infection risk for susceptible individuals decreases due to the large number of passengers seated in each row, and the probability of airborne infection risk for susceptible individuals is zero when no passengers are seated in each row.

In Figure 18, we show the probability of airborne infection risk for susceptible individuals every 10 minutes. At 10 minutes and 40 minutes, there are fewer passengers in each row, so there is a greater likelihood of infection. Where 20 minutes and 30 minutes are at low risk of infection due to the greater number of passengers in each row, the probability of airborne infection risk for susceptible individuals every 10 minutes is shown in Table VI.

VI. Conclusion

A numerical mathematical model is utilized to predict the risk of airborne infection on a ventilated bus. The concentration of carbon dioxide, the volume fraction of exhaled air, the concentration of airborne infectious particles, the number of airborne infectious particles, and the probability of airborne infection risk for susceptible individuals all change as the number of passengers in each cycle and the ventilation rate change. We demonstrate the applicability of the suggested technique to real-world issues by employing explicit finite difference techniques to approximate the model's solution. The proposed air quality model was found to be in good agreement in that it allows us to know the balance between the number of passengers allowed to sit on the bus while managing the risk of airborne infection, carbon dioxide concentration, and ventilation system potential. Better air quality control that achieves a balance between the number of passengers allowed to ride in a bus will be a significant advantage of the ventilation. The proposed model can be modified to consider two or three-dimensional domains.

References

[1] J.R. Andrews, C. Morrow, and R. Wood, "Modeling the role of public transportation in sustaining tuberculosis transmission in South Africa am," *American Journal of Epidemiology*, vol. 177, no. 6, pp. 556-561, 2012.

[2] W.F. Well, "Airborne contagion and air hygiene. An ecological study of droplet infections," 1955.

[3] S.N. Rudnick and D.K. Milton, "Risk of indoor airborne infection transmission estimated from carbon dioxide concentration," *Indoor Air*, vol. 13, no. 3, pp. 237-245, 2003.

[4] E.T. Richardson, C.D. Morrow, D.B. Kalil, and L.G. Bekker, "Shared air: a renewed focus on ventilation for the prevention of tuberculosis transmission," *PloS One*, vol. 9, no. 5, 2014.

[5] L. Gammaitioni and M.C. Nucci, "Using a mathematical model to evaluate the efficacy of TB control measures," *Emerging Infectious Diseases*, vol. 13, no. 3, pp. 335-342, 1997.

[6] S.J. Emmerich and A.K. Persily, "State-of-the-art review of carbon dioxide bemand controlled ventilation technology an application," *NISTIR 6729*, 2001.

[7] Y. Li, G.M. Leung, J.W. Tang, X. Yang, C.Y.H. Chao, J.Z. Lin, and P.L. Yuen, "Role of ventilation in airborne transmission of infectious agents in the built environmental multidisciplinary systematic review," *Indoor Air*, vol. 17, no. 1, pp. 2-18, 2007.

[8] M. Murray, O. Oxlade, and H.H. Lin, "Modeling social, environmental, and biological determinants of tuberculosis," *The International Journal of Tuberculosis and Lung Disease*, vol. 15, no. 6, pp. S64-S70, 2011.

[9] A.K. Persily, "Evaluating building IAQ and ventilation with indoor carbon dioxide," *Transactions-American Society of Heating Refrigerating and Air Conditioning Engineers*, no. 103, pp. 193-204, 1997.

[10] M. Lygizos, S.V. Shenoi, B.P. Brooks, A. Bhushan, J.C. Brust, D. Zeltenman, and G.H. Friedland, "Natural ventilation reduces high tb transmission risk in traditional homes in rural Kwazulu-Natal, South Africa," *BMC Infectious Disease*, vol. 13, no. 1, pp. 1-8, 2013.

[11] H.L. Rieder, "Socialization pattens are key to the transmission dynamics of tuberculosis," *The International Journal Tuberculosis Lung Disease*, vol. 3, no. 3, pp. 177-178, 1999.

[12] H.L. Rieder, "Epidemiological Basis of Tuberculosis Control," no. ed. 1, pp. 1-162, 1999.

[13] R.G. London and R.M. Roberts, "Droplet expulsion from the respiratory tract," *American Review of Respiratory Disease*, vol. 95, no. 3, pp. 435-442, 1967.

[14] C.B. Beggs, C.J. Noakes, P.A. Fletcher, and K. Siddiqi, "The transmission of tuberculosis in confined spaces: an analytical review of alternative epidemiological models," *The International Journal Tuberculosis Lung Disease*, vol. 7, no. 11, pp. 1015-1026, 2003.

[15] G.N. Sze To and C.Y.H. Chao, "Review and comparison between the wells-Riley and dose-response approaches to risk assessment of infections respiratory diseases," *Indoor Air*, vol. 20, no. 1, pp. 2-16, 2010.

[16] K. Suebyat, P. Oyjinda, S.A. Konglok, and N. Pochai, "A mathematical model for the risk analysis of airborne infectious disease in an Outpatient room with personal classification factor," *Engineering Letters*, vol. 28, no. 4, pp. 1331-1337, 2020.

[17] C.J. Noakes and P.A. Sleigh, "Mathematical models for assessing the role of airflow on the risk of airborne infection in hospital wards," *Journal of The Royal Society Interface*, vol. 6, no. suppl 6, pp. S791-S800, 2009.

[18] R. Wood, C.Morrow, S.Ginsberg, E.Piccoli, D. Kalil, A.Sassi, and J.R. Andrews, "Quantification of shared air: a social and environmental determinant of airborne disease transmission," *PloS One 9*, vol. 9, no. 9, 2014.

[19] T. L. R. Medicine, "COVID-19 transmission—up in the air," *The Lancet Respiratory Medicine*, vol. 8, no. 12, 2020.

[20] S. Farooq, F. Zubair, and M.A. Kamal, "Evaluation of ventilation system efficiency with reference to ceiling height in warm-humid climate of Pakistan," *Civil Engineering and Architecture*, vol. 8, no. 5, pp. 824-831, 2020.

[21] M.I. Chacha, M. Nicola, and W. Robin, "Modelling the risk of airborne infectious disease using exhaled air," *Journal of Theoretical Biology*, vol. 372, pp. 100-106, 2015.

[22] W. Timpitak and N. Pochai, "A numerical model of carbon dioxide concentration measurement in a room with an opened ventilation system," *Environment and Ecology Research*, vol. 9, no. 3, pp. 107-113, 2021.

[23] CF. Dillon and MB. Dillon, "Multiscale airborne infectious disease transmission," *Applied and Environmental Microbiology*, vol. 87, no. 4, 2021.

[24] T. Lipinski, D. Ahmad, N. Serey, and H. Jouhara, "Review of ventilation strategies to reduce the risk of disease transmission in high occupancy buildings," *International Journal of Thermofluids*, vol. 7-8, 100045, 2020.
[25] L. Morawska and J. Cao, "Airborne transmission of SARS-CoV-2: The world should face the reality," *Environment International*, vol. 139, 105730, 2020.
[26] A.R. Mitchell, "Computational methods in partial differential equations," Public Wiley, New York, 1969.
[27] W. Timpitak and N. Pochai, "A mathematical model of risk assessment on airborne infection in a room with an outlet ventilation system," *Engineering Letters*, vol. 30, no. 2, pp. 898-903, 2022.
[28] W. Boonmeemapasuk and N. Pochai, "A risk model of airborne transmission and vaccine efficacy in an outpatient room with a ventilation system," *Engineering Letters*, vol. 30, no. 2, pp. 644-651, 2022.
[29] H. Thongzunhor and N. Pochai, "A three-dimensional air quality measurement model in an opened high traffic street canyon using an explicit finite difference method," *Engineering Letters*, vol. 29, no. 3, pp. 996-1004, 2021.
[30] P. Othata and N. Pochai, "A mathematical model of salinity control in a river with an effect of internal waves using two explicit finite difference methods," *Engineering Letters*, vol. 29, no. 2, pp. 689-696, 2021.
[31] P. Othata and N. Pochai, "Irrigation water management strategies for salinity control in the chao phraya river using sualyev finite difference method with lagrange interpolation technique," *Engineering Letters*, vol. 29, no. 2, pp. 332-338, 2021.
[32] P. Unyapoti and N. Pochai, "A shoreline evolution model with a twin groins structure using unconditionally stable explicit finite difference techniques," *Engineering Letters*, vol. 29, no. 1, pp. 288-296, 2021.
[33] P. Unyapoti and N. Pochai, "A shoreline evolution model with the wavelength effect of breaking waves on groin structure," *IAENG International Journal of Computer Science*, vol. 49, no. 3, pp. 683-694, 2022.
[34] N. Pongnu and N. Pochai, "Mathematical modelling of groundwater quality measurement around a landfill for residential water usage," *Engineering Letters*, vol. 30, no. 3, pp. 1006-1016, 2022.
[35] W. Klaychang and N. Pochai, "Implicit finite difference simulation of water pollution control in a connected reservoir system," *IAENG International Journal of Applied Mathematics*, vol. 46, no. 1, pp. 47-57, 2016.
[36] S.A. Konglok and N. Pochai, "Numerical computations of three-dimensional air-quality model with variations on atmospheric stability classes and wind velocities using fractional step method," *IAENG International Journal of Applied Mathematics*, vol. 46, no. 1, pp. 112-120, 2016.

J. Sooknum is an assistant researcher of Centre of Excellence in Mathematics, MHESI, Bangkok 10400, Thailand.

N. Pochai is a researcher of Centre of Excellence in Mathematics, MHESI, Bangkok 10400, Thailand